ACS APPLIED MATERIALS & INTERFACES

Research Article

www.acsami.org

Zinc Oxide Nanowire Photodetectors with Single-Walled Carbon Nanotube Thin-Film Electrodes

Elif Selen Ates,[†,§] Seyda Kucukyildiz,[†,§] and Husnu Emrah Unalan*[,†,‡]

[†]Department of Metallurgical and Materials Engineering, Middle East Technical University, Ankara 06800, Turkey

[‡]Center for Solar Energy Research and Applications, Middle East Technical University, Ankara 06800, Turkey

Supporting Information

ABSTRACT: In this study, transparent and flexible zinc oxide (ZnO) nanowire ultraviolet (UV) photodetectors prepared via a solution-based method in which single-walled carbon nanotube (SWNT) thin films were used as transparent electrodes are reported. The photoresponse current was found to be in proportion with the ZnO nanowire density, and the nanowire density could be tuned to increase the photocurrent by a factor of 300. The decay time for the fabricated photodetectors was found to be as low as 16 s. This study suggests the possibility of fabricating inexpensive, visible-blind UV photodetectors via solution-based methods.

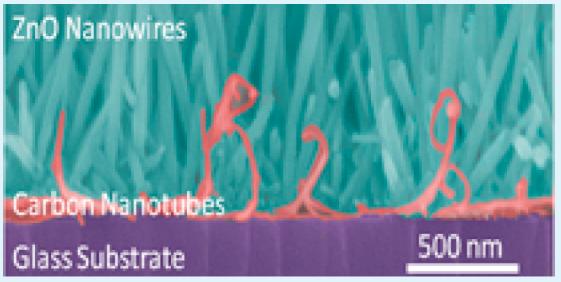

KEYWORDS: *carbon nanotubes, zinc oxide, nanowires, photodetectors, heterojunctions, transparent and flexible devices*

INTRODUCTION

UV exposure has become more pronounced as the size of the ozone hole in the Antarctic stratosphere increases, which may be dangerous to human health. UV radiation causes the generation of free-radical chemical species[1] that participate in the development of various pathologies, such as cancer, aging, Alzheimer's disease, inflammatory disorders, and other ailments.[2] Therefore, UV photodetectors play an important role in monitoring UV radiation that has implications for human health. In addition to biological and chemical sensors, other important application fields of UV photodetectors include fire detection, optical intersatellite spatial communications, the calibration of emitters, and UV imaging.[3]

Nanoscale UV photodetectors offer flexibility and transparency in the visible regime. For this purpose, one-dimensional wide-bandgap semiconductor nanostructures have been preferred. Among them, ZnO, which exhibits a direct wide bandgap (3.37 eV) and a large exciton binding energy (60 meV), is a promising candidate for use in photodetectors[4] and other optoelectronic devices, such as sensors,[5] solar cells,[6] and light-emitting diodes.[7]

Because of their fast response and recovery,[8] cost-effective fabrication procedures,[9] and high on/off ratio,[10] ZnO nanowires (NWs) are candidates for active materials in UV sensors. Numerous researchers have reported UV photodetectors that incorporate ZnO nanowires; however, most of these photodetectors were fabricated using high-vacuum and high-temperature processes, such as chemical vapor deposition, thermal evaporation, and sputtering.[11,12,4,13]

To fabricate a fully transparent and flexible device, both the active element and the contacts must individually exhibit these characteristics. Single-walled carbon nanotube (SWNT) thin films have already been used as transparent electrodes in optoelectronic devices, including solar cells,[6] organic light-emitting diodes (OLEDs),[14] photodetectors,[15−17] and electrochromic devices,[18] among others,[19−21] because of their remarkable optoelectronic and chemical properties.[14,22] These unique one-dimensional structures are also preferred in flexible electronics because of their outstanding mechanical properties and ability to form homogeneous networks.[23,24] They have shown a fascinating ability to form large-area, conductive, transparent thin films on different substrates.[25,26]

In the recent past, heterojunctions between SWNTs and various metal oxides, such as V_2O_4,[27] SnO_2,[28] TiO_2,[29] ZnO,[30] and MnO_2,[31] in different morphologies have been the subject of intense interest with respect to their functionalities. ZnO/SWNT composite structures were one of these technologically attractive combinations, and they were investigated for their optoelectronic properties. For example, hybrid structures composed of ZnO nanoparticles and carbon nanotubes have been investigated with respect to their potential applications in ultrafast nonlinear optical switching,[32] flexible organic photovoltaics,[6] and UV photodetectors.[30,33]

In this investigation, we have fabricated and characterized metal−semiconductor−metal (MSM) photodetectors on rigid glass and flexible polyethylene terephthalate (PET) substrates utilizing solution-based, low-cost methods. For this purpose, hydrothermally grown ZnO nanowires and solution-deposited SWNT thin films were used for the active layer and the electrodes, respectively. The performance of flexible samples was comparable to those fabricated on rigid substrates. The effect of ZnO nanowire density was also investigated.

Received: June 4, 2012
Accepted: September 5, 2012
Published: September 5, 2012

 © 2012 American Chemical Society dx.doi.org/10.1021/am301402y | *ACS Appl. Mater. Interfaces* 2012, 4, 5142−5146

EXPERIMENTAL DETAILS

All chemicals were purchased from Sigma-Aldrich and used without further purification. SWNT thin-film electrodes were deposited prior to the growth of ZnO nanowires. The deposition procedure has been reported elsewhere.[34] In brief, purified SWNTs were purchased from Carbon Solutions, Inc., and a stable, sodium dodecyl sulfate (SDS)-assisted SWNT dispersion was prepared in deionized water (18.3 MΩ). The SWNT solution was sonicated at 20 kHz using a tip sonicator and was subsequently vacuum filtered onto mixed cellulose ester (MCE) membranes. After filtration, the MCE membranes were transferred onto soda-lime silica glass and PET substrates via compressive loading and drying at 80 °C for 2 h. Finally, the membranes were dissolved by consecutive washing with acetone (99.8%) and isopropyl alcohol (99.8%). The SWNT thin films were treated with nitric acid (HNO_3, 65%) for 3 h. After this treatment, the measured sheet resistance and transparency values of the films were 100 Ω/sq and 90%, respectively.

After the deposition of SWNT thin films onto glass and PET substrates, a gap was introduced by mechanical means using a razor blade. The size of the gap was measured to be 30 μm. ZnO nanowires were synthesized within these gaps. For the synthesis of the ZnO nanowires, a seed solution was first prepared by dissolving 10 mM zinc acetate dihydrate ($Zn(C_2H_3O_2)_2{\cdot}2H_2O$, extra pure) in 1-propanol. The substrates were subsequently covered with this solution by spin coating the seed solution at 2000 rpm. The number of spin-coating cycles is known to control the nanowire density, and various spin-coating repetitions were performed to investigate the effects of nanowire density on the photocurrent. The seeded substrates were then dried on a hot plate at 100 °C. This heating process was repeated after each spin-coating cycle.

The nanowire growth solution was prepared in deionized water with an equimolar (25 mM) mixture of zinc acetate dihydrate and hexamethylenetetramine (HMTA). The seeded substrates were placed vertically within this growth solution in a Teflon holder. The solution was subsequently submerged into a silicon oil bath set at 90 °C. After 2 h, the substrates were removed from the growth solution, rinsed with deionized water, and dried under flowing nitrogen. The morphology of the nanowires was investigated by field-emission scanning electron microscopy (FESEM) (Nova Nano-SEM 430), and the density of the nanowires was calculated from the obtained images. Photocurrent measurements were performed using a constant dc bias of 2 V through a Keithley 2400 source meter. A UV lamp with a wavelength and power density of 365 nm and 1 mW/cm^2, respectively, was used as the UV source. Silver dag was used for the connections. Spectral responsivity measurements of the photodetectors were performed using a Newport Oriel Apex Monochromator Illuminator equipped with a halogen-lamp light source.

RESULTS AND DISCUSSION

A schematic of the fabricated devices is provided in Figure 1a. For the fabrication of the photodetectors, ZnO nanowires were grown on and between the gaps of the SWNTs, as shown in the SEM image in Figure S1 in the Supporting Information.

Detailed SEM examination revealed that as the number of spin-coating repetitions was increased, the length and diameter of the ZnO NWs decreased, whereas the ZnO nanowire density increased. The calculated nanowire densities were 1, 30, 70, and 100 NW/μm^2, which correspond to 1, 3, 5, and 10 spin-coating sequences, respectively. Top-view SEM images of the ZnO nanowires with different densities are provided in Figure S2 in the Supporting Information. Top and cross-sectional SEM images of the device with a nanowire density of 100 NW/μm^2 are shown in parts b and c of Figure 1, respectively. The SWNT bundles underneath ZnO nanowires are clearly evident in the false-colored SEM image.

The normal incidence transmittance of the fabricated devices in the 400−800 nm wavelength range is shown in Figure 2a.

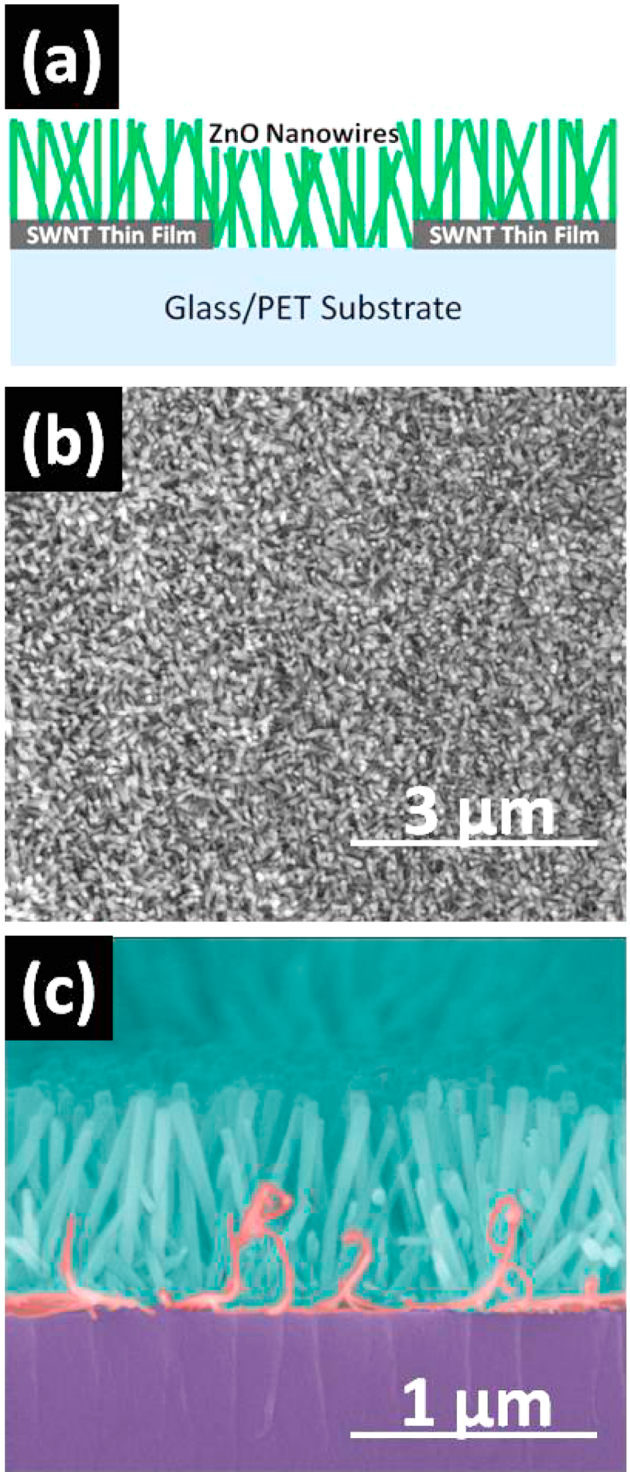

Figure 1. (a) Schematic of the fabricated devices. (b) Top-view SEM image of ZnO nanowires grown within the gap of SWNT thin-film electrodes. (c) False colored, cross-sectional SEM image of ZnO nanowires grown on top of the SWNT thin-film electrodes.

For comparison, the transmittance of the bare SWNT thin film is also provided in the same figure. The transmittance values at 550 nm were 82%, 81%, 71%, and 69% for the devices with nanowire densities of 1, 30, 70, and 100 NW/μm^2, respectively. The transmittance values of the devices were found to be inversely proportional to the nanowire density because the amount of light scattering increased with increasing density of

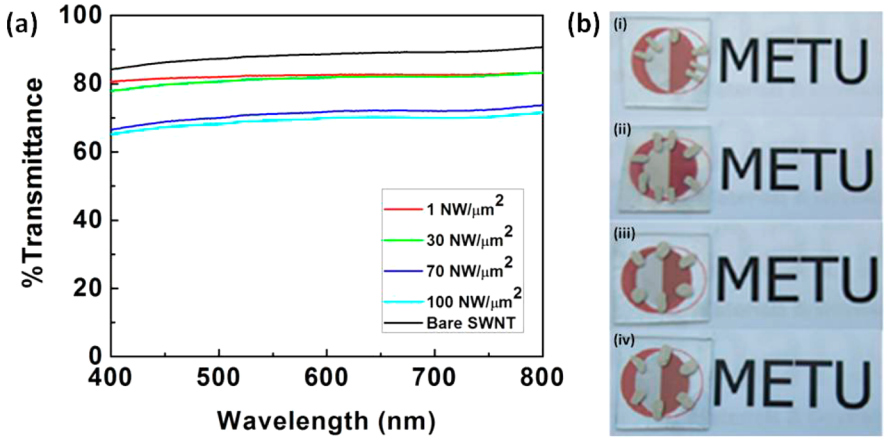

Figure 2. (a) Transmittance spectra of the ZnO photodetectors with different nanowire densities. (b) Photographs of the ZnO photodetectors with nanowire densities of (i) 1, (ii) 30, (iii) 70, and (iv) 100 NW/μm^2.

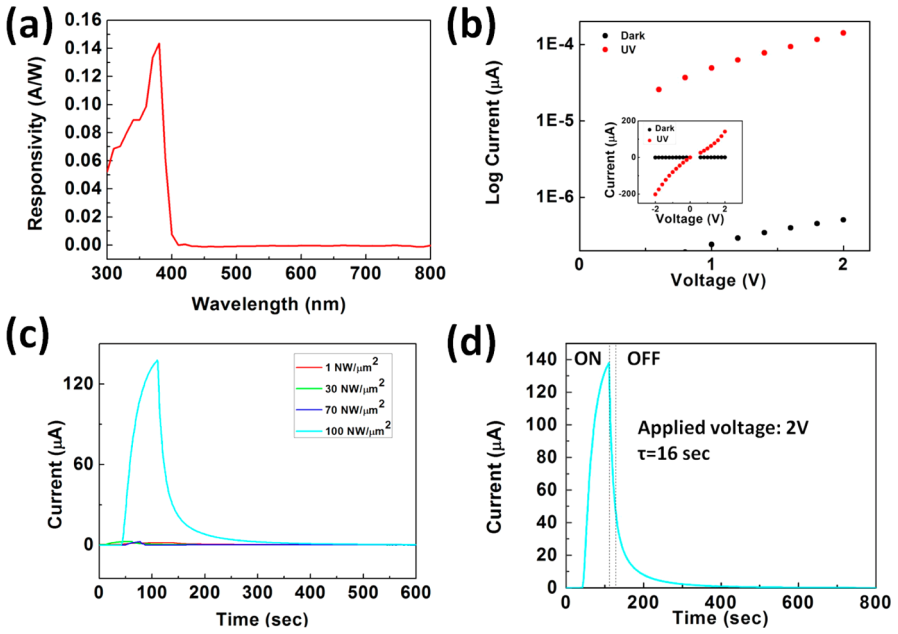

Figure 3. The (a) spectral response and (b) current–voltage characteristics of a ZnO nanowire photodetector plotted on a logarithmic scale (under dark and UV irradiance). The inset shows the current–voltage characteristics under dark conditions and under UV irradiation of a ZnO nanowire photodetector. (c) Photoresponse of the ZnO photodetectors with different nanowire densities under UV irradiation and a bias voltage of 2 V. (d) Response and recovery current curve at an applied bias of 2 V.

the ZnO NWs. Photographs of the fabricated devices with different nanowire densities are shown in Figure 2b. The fabricated devices exhibit adequate transparency even at high nanowire densities, and the logos behind the devices are therefore apparent.

The UV photoresponse current (ΔI) is defined as the difference between the photoresponse current under UV illumination (I) and the dark current (I_0). For UV photodetectors composed of multiple nanowires, the photoresponse current should linearly increase with the number of nanowires. In this case, the photoresponse current is defined as $\Delta I = \Sigma(I - I_0)$. To investigate the dependence of the UV photoresponse on the nanowire density, the UV photoresponse currents were measured for four different devices with different nanowire densities. The photoresponse currents of the devices were 1.9, 3.4, 9, and 520 μA for devices with nanowire densities of 1, 30, 70, and 100 NW/μm^2, respectively. The photoresponse current increased nonlinearly with the nanowire density, which may be due to an increase in the percolating current pathways above some threshold density. Moreover, the number of ZnO nanowires increases the number of charge carriers, which could lead to an increase in the photoresponse.

Spectral response is defined as the ratio between the current generated by the photodetector and the power of the incident light on the photodetector. Semiconductors cannot absorb photons with the energies less than their band-gap energy. This phenomenon was confirmed by the typical spectral response of the ZnO nanowire UV photodetector at a forward bias of 2 V (Figure 3a). A sharp cutoff in the responsivity of the fabricated photodetectors was observed at wavelengths greater than 380 nm, which is near the band-edge absorption of ZnO. UV light with energies greater than the bandgap of the ZnO were absorbed by the ZnO and generated electron–hole pairs that contributed to the photocurrent. This contribution resulted in a response to the UV light. Spectral response measurements

dx.doi.org/10.1021/am301402y | ACS Appl. Mater. Interfaces 2012, 4, 5142–5146

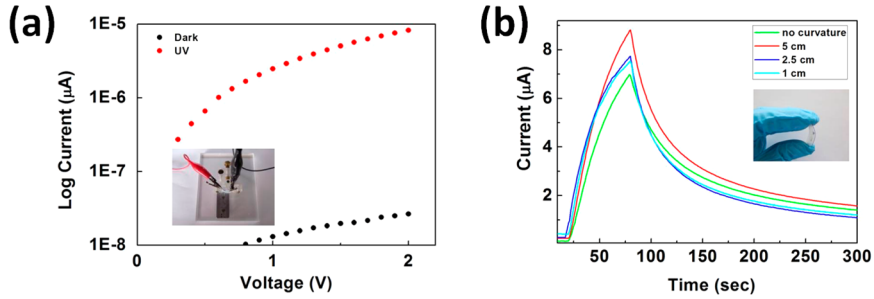

Figure 4. (a) Current–voltage characteristics, plotted on a natural logarithmic scale, of the flexible devices under dark conditions and under UV irradiation. (b) Response and recovery-current characteristics of the fabricated flexible and transparent ZnO nanowire photodetectors. The inset shows a photograph of the fabricated photodetector.

clearly indicated the visible-blind nature of the fabricated detectors.

Current–voltage characteristics of a fabricated photodetector with a nanowire density of 100 NW/μm^2 measured under dark and illuminated conditions on a log-scale are shown in Figure 3b. The inset shows the current–voltage characteristics on a linear scale. Notably, we reproducibly obtained similar device characteristics. The measured current increased in proportion with the applied bias for all four samples. The response current was symmetric and quasi-linear, which indicates that highly resistant nanowire–nanowire junctions instead of ohmic nanowire–electrode junctions dominated the conduction.

Variations of the photoresponse current with time for those four devices are shown in Figure 3c. As a result of the proportionality with the nanowire density, the device with a nanowire density of 100 NW/μm^2 appears to overpower the others. Under an applied bias of 2 V, the dark current and photocurrent of this device were 2×10^{-9} and 5.2×10^{-4} A, respectively, which yielded an on/off current ratio of 260 000; this ratio is quite promising when compared to values reported in the literature.[35,36] Moreover, the on/off current ratios of the devices with the nanowire densities of 1, 30, 70 NW/μm^2 were 242, 1504 and 2055, respectively. Thus, the on/off current ratio is proportional to the nanowire density. To investigate the photoresponse process in detail, the recovery times (τ) of the samples were investigated. Recovery time is defined as the time required for the photocurrent to decrease from its steady-state value to a value that is 36.8% of the steady-state value.[35] The device with a nanowire density of 100 NW/μm^2 exhibited a recovery time of approximately 16 s (Figure 3d), which is relatively poor compared to those of optimized photodetectors with CVD-grown nanowires[13] and Schottky-barrier devices;[37] however, this time is significantly shorter than the recovery time of the devices fabricated with ZnO nanowires that were synthesized using similar methods.[11,38] The recovery time of the devices with nanowire densities of 70, 30, and 1 NW/μm^2 were calculated to be 24, 28, and 56 s, respectively. The adsorption and desorption of oxygen has been observed to control the photoresponse process.[39] Under dark conditions, oxygen molecules adsorbed on the surface of ZnO nanowires trap free electrons of the n-type semiconductor [$O_2 + e^- \rightarrow O_2^-(ad)$]. This trapping decreases the carrier density in the nanowires and the mobility of the remaining electrons by creating depletion layers near the surface. Because of their large surface-to-volume ratio, the adsorption of O_2 significantly decreases the conductivity of the nanowires. Upon UV illumination, electron and hole pairs are generated [$h\upsilon \rightarrow e^- + h^+$]. These photocarriers immediately increase the conductivity because of the sudden increase in the nanowire carrier density. Holes migrate to the surface and recombine with the oxygen-trapped electrons and release the O_2^- from the surface [$O_2^-(ad) + h^+ \rightarrow O_2(g)$]. The remaining unpaired electrons became major carriers and contribute to the current until they are trapped again by readsorbed O_2 on the surface. The photocurrent increases gradually under UV illumination until desorption and readsorption of O_2 reach an equilibrium state. When the UV illumination is stopped, holes recombine with electrons; however, numerous electrons still remain in the nanowires because, at the end of the illumination, the hole density is significantly lower than the electron density in the nanowires. The O_2 molecules are readsorbed onto the surface and trap the remaining unpaired electrons. As a result of the large number of these unpaired electrons, the current decay slows and the recovery time increases. The decrease in the recovery time with increasing nanowire density can be explained by this phenomenon. Oxygen adsorption increases with increasing nanowire density; thus, the recovery time becomes shorter.

The photoresponse characteristics of the devices fabricated on flexible PET substrates were also measured. Ohmic contact between the SWNT thin film electrodes and the ZnO nanowires on PET substrates was confirmed by current–voltage measurements, as shown in Figure S3 in the Supporting Information. The results of these measurements plotted on a log scale are shown in Figure 4a. The measured current increased in proportion to the applied bias for the flexible devices. A picture of the measurement setup is provided in the inset of Figure 4a. The performances of these devices under strain while bent to different radii of curvature were investigated. A typical photoresponse of as-fabricated and strained devices are provided in Figure 4b. A picture of one of the fabricated flexible photodetectors is given in the inset. Effective photodetection under various bending conditions have been obtained. The increase in the photocurrent when the substrate was bent to different radii of curvature can be attributed to the improved mechanical coupling between the SWNT electrodes and the ZnO nanowires.

Transparent and flexible devices primarily offer mobility to the end user. They can be simply integrated into various platforms for detection, such as in the case of sensors. In addition, photodetectors formed by the heterojunctions between SWNT thin films and ZnO nanowires can be deposited over large areas through simple, straightforward, and room-temperature processes. In contrast to the ensemble behavior of the SWNTs and ZnO nanowires, effective visible-

blind photodetection for both devices on glass and PET substrates was obtained.

In conclusion, we have demonstrated an inexpensive, solution-based approach to the fabrication of transparent and flexible ZnO nanowire visible-blind UV photodetectors using SWNT thin-film electrodes. Controlled experiments were conducted to investigate the relationship between the photoresponse current and the nanowire density. The experiments showed that the photoresponse current increased with increasing nanowire density as a result of an increased number of charge carriers. A recovery time as low as 16 s was obtained for the fabricated photodetectors. In addition, the transparent and flexible UV photodetectors showed nearly unchanged performance upon being bent to different radii of curvature. Our results revealed the potential of SWNT and ZnO nanowire junctions to be used as simple yet efficient UV photodetectors. The results acquired in this investigation for the SWNT and ZnO nanowire heterojunctions reveal their potential for various other optoelectronic devices.

■ ASSOCIATED CONTENT

Ⓢ Supporting Information

SEM images of the fabricated photodetectors showing the contacts and the channel region and SEM images of nanowires with different densities and dark current−voltage characteristics for devices fabricated on PET substrates. This material is available free of charge via the Internet at http://pubs.acs.org.

■ AUTHOR INFORMATION

Corresponding Author

*E-mail: unalan@metu.edu.tr.

Author Contributions

[§]Authors contributed equally to this work.

Notes

The authors declare no competing financial interest.

■ ACKNOWLEDGMENTS

This work was supported by the Scientific and Technological Research Council of Turkey (TUBITAK) under Grant Nos. 109M084 and 109M487 and the Distinguished Young Scientist Award of the Turkish Academy of Sciences (TUBA).

■ REFERENCES

(1) Black, H. S. *J. Invest. Dermatol.* **2004**, *122*, 13−14.
(2) Liebler, D. C. *Chem. Res. Toxicol.* **2006**, *19*, 610−613.
(3) Omnes, F.; Monroy, E. In *Optoelectronic Sensors*, 1st ed.; Decoster, D., Harari, J., Eds.; John Wiley & Sons: Hoboken, NJ, 2009; p 181.
(4) Soci, C.; Zhang, A; Xiang, B.; Dayeh, S. A; Aplin, D. P. R.; Park, J.; Bao, X. Y.; Lo, Y. H.; Wang, D. *Nano Lett.* **2007**, *7*, 1003−1009.
(5) Lim, Z. H.; Chia, Z. X.; Kevin, M.; Wong, A. S. W.; Ho, G. W. *Sens. Actuators, B* **2010**, *151*, 121−126.
(6) Unalan, H. E.; Hiralal, P.; Kuo, D.; Parekh, B.; Amaratunga, G.; Chhowalla, M. *J. Mater. Chem.* **2008**, *18*, 5909−5912.
(7) Könenkamp, R.; Word, R. C.; Schlegel, C. *Appl. Phys. Lett.* **2004**, *85*, 6004.
(8) Trinchi, A.; Galatsis, K.; Wlodarski, W.; Li, Y. X. *IEEE Sens. J.* **2003**, *3*, 548−553.
(9) Greene, L. E.; Yuhas, B. D.; Law, M.; Zitoun, D.; Yang, P. *Inorg. Chem.* **2006**, *45*, 7535−7543.
(10) Lao, C. S.; Park, M.-Chul; Kuang, Q.; Deng, Y.; Sood, A. K.; Polla, D. L.; Wang, Z. L. *J.Am. Chem. Soc.* **2007**, *129*, 12096−12097.
(11) Zhou, H.; Fang, G.; Liu, N.; Zhao, X. *Nano. Res. Lett.* **2011**, *6* (147), 1−6.
(12) Hsu, C.-L.; Chang, S.-J.; Lin, Y.-R.; Li, P.-C.; Lin, T.-S.; Tsai, S.-Y.; Lu, T.-H.; Chen, I.-C. *Chem. Phys. Lett.* **2005**, *416*, 75−78.
(13) Cheng, G.; Wu, X.; Liu, B.; Li, B.; Zhang, X.; Du, Z. *Appl. Phys. Lett.* **2011**, *99*, 203105.
(14) Li, J.; Hu, L.; Wang, L.; Zhou, Y.; Gruner, G.; Marks, T. J. *Nano Lett.* **2006**, *6*, 2472−2477.
(15) Chang, J; Najeeb, C.K.; Lee, J. -H.; Lee, M; Kim, J.-H. *J. Phys. D: Appl. Phys.* **2011**, *44*, 095101.
(16) Behnam, A.; Johnson, J.; Choi, Y.; Noriega, L.; Ertosun, M. G.; Wu, Z.; Rinzler, A. G.; Kapur, P.; Saraswat, K. C.; Ural, A. *J. Appl. Phys.* **2008**, *103*, 114315.
(17) Ambrosio, M.; Ambrosio, a.; Ambrosone, G.; Campajola, L.; Cantele, G.; Carillo, V.; Coscia, U.; Iadonisi, G.; Ninno, D.; Maddalena, P.; Perillo, E.; Raulo, a.; Russo, P.; Trani, F.; Esposito, E.; Grossi, V.; Passacantando, M.; Santucci, S.; Allegrini, M.; Gucciardi, P. G.; Patanè, S.; Bobba, F.; Di Bartolomeo, A.; Giubileo, F.; Lemmo, L.; Scarfato, A.; Cucolo, A. M. *Nucl. Instrum. Methods Phys. Res., Sect. A* **2009**, *610*, 1−10.
(18) Hu, L.; Gruner, G.; Li, D.; Kaner, R. B.; Cech, J. *J. Appl. Phys.* **2007**, *101*, 016102.
(19) Chen, H.; Xi, N.; Lai, K. W. C.; Fung, C. K. M.; Yang, R. *IEEE Trans. Nano* **2010**, *9*, 582−589.
(20) Unalan, H. E.; Fanchini, G.; Kanwal, A.; Du Pasquier, A.; Chhowalla, M. *Nano Lett.* **2006**, *6*, 677−682.
(21) Yu, X.; Rajamani, R.; Stelson, K. A.; Cui, T. *Sens. Actuators, A* **2006**, *132*, 626−631.
(22) Zhang, D.; Ryu, K.; Liu, X.; Polikarpov, E.; Ly, J.; Tompson, M. E.; Zhou, C. *Nano Lett.* **2006**, *6*, 1880−1886.
(23) Ou, E. C.-W.; Hu, L.; Raymond, G. C. R.; Soo, O. K.; Pan, J.; Zheng, Z.; Park, Y.; Hecht, D.; Irvin, G.; Drzaic, P.; Gruner, G.; Soo, O. K.; Pan, J.; Zheng, Z.; Park, Y.; Hecht, D.; Irvin, G.; Drzaic, P.; Gruner, G. *ACS Nano* **2009**, *3*, 2258−2264.
(24) Sreekumar, T. V.; Liu, T.; Kumar, S.; Ericson, L. M.; Hauge, R. H.; Smalley, R. E. *Chem. Mater.* **2003**, *15*, 175−178.
(25) Soetedjo, H.; Mora, M. F.; Garcia, C. D. *Thin Solid Films* **2010**, *518*, 3954−3959.
(26) Song, Y. I.; Yang, C.-M.; Kim, D. Y.; Kanoh, H.; Kaneko, K. *J. Colloid Interface Sci.* **2008**, *318*, 365−371.
(27) Willinger, M.-G.; Neri, G.; Rauwel, E.; Bonavita, A.; Micali, G.; Pinna, N. *Nano Lett.* **2008**, *8*, 4201−4204.
(28) Kuang, Q.; Li, S.; Xie, Z.; Lin, S.; Zhang, X.; Xie, S.; Huang, R.; Zheng, L. *Carbon* **2006**, *44*, 1166−1172.
(29) Xia, X.; Jia, Z.; Yu, Y.; Liang, Y.; Wang, Z.; Ma, L. *Carbon* **2007**, *45*, 717−721.
(30) Dutta, M.; Basak, D. *Chem. Phys. Lett.* **2009**, *480*, 253−257.
(31) Chen, P.-C; Shen, G.; Shi, Y.; Chen, H.; Zhou, C. *ACS Nano* **2010**, *4*, 4403−4411.
(32) Zhu, Y.; Elim, H. I.; Foo, Y.-L.; Yu, T.; Liu, Y.; Ji, W.; Lee, J.-Y.; Shen, Z.; Wee, A. T. S.; Thong, J. T. L.; Sow, C. H. *Adv. Mater.* **2006**, *18*, 587−592.
(33) Lin, Y.-H.; Lee, P.-S.; Hsueh, Y.-C.; Pan, K.-Y.; Kei, C.-C.; Chan, M.-H.; Wu, J.-M.; Perng, T.-P.; Shih, H. C. *J. Electrochem. Soc.* **2011**, *158*, K24−K27.
(34) Wu, Z.; Chen, Z.; Du, X.; Logan, J. M.; Sippel, J.; Nikolou, M.; Kamaras, K.; Reynolds, J. R.; Tanner, D. B.; Hebard, A. F.; Rinzler, A. G. *Science* **2004**, *305*, 1273−1276.
(35) Bai, S.; Wu, W.; Qin, Y.; Cui, N.; Bayerl, D. J.; Wang, X. *Adv. Func. Mater.* **2011**, *21*, 4464−4469.
(36) Jung, B. O.; Kim, D. C.; Kong, B. H.; Kim, D.-W.; Cho, H. K. *Sens. Actuators, B* **2011**, *160*, 740−746.
(37) Jin, Y.; Wang, J.; Sun, B.; Blakesley, J.C.; Greenham, N.C. *Nano Lett.* **2008**, *8*, 1649−1653.
(38) Liu, N.; Fang, G.; Zeng, W.; Zhou, H.; Cheng, F.; Zheng, Q.; Yuan, L.; Zou, X.; Zhao, X. *ACS Appl. Mater. Interfaces* **2010**, *2*, 1973−1979.
(39) Li, Y.; Della Valle, F.; Simonnet, M.; Yamada, I.; Delaunay, J.-J. *Appl. Phys. Lett.* **2009**, *94*, 023110.